ELSEVIER

Journal of Nuclear Materials 258–263 (1998) 777–781

journal of nuclear materials

Modelling of tritium permeation through beryllium as plasma facing material

L. Berardinucci *

Forschungszentrum Karlsruhe, Institut für Neutronenphysik und Reaktortechnik (INR), Postfach 3640, D-76021 Karlsruhe, Germany

Abstract

Due to a number of technological properties and, first of all, to a low atomic number, beryllium will be used as plasma facing material in ITER. Tritium control, including both the permeation through and inventory in the beryllium, is of great importance for the safety of the device. Experimental data have shown that, under ITER-like plasma conditions, the plasma facing surfaces of the beryllium develop high porosity (bubbles) and become saturated with bubbles, leading to a strong uptake of tritium and deuterium ions almost independent of the incident flux. At fluxes typical of ITER, surface erosion of beryllium should be also taken into account. A computational model has been used with the computer code TMAP4 to reproduce the available experimental data concerning hydrogen ion implantation in beryllium. The results described in this paper refer to the first wall of the European Helium Cooled Pebble Bed Blanket (HCPB) Test Blanket Module (TBM-I).

1. Introduction

The European Fusion Programme proposes two DEMO relevant blanket concepts for testing in ITER: the Water Cooled Lithium Lead (WCLL) blanket and the Helium Cooled Pebble Bed (HCPB) blanket. Both use martensitic steel as structural material. Results here presented concerning the tritium control cover the design specifications of the HCPB TBM-I [1]. In the HCPB reference design [1–3], the breeder and the neutron multiplier consist of separate beds of Li_4SiO_4 and beryllium pebbles, respectively. These beds are contained between steel plates cooled by high pressure helium. The tritium produced in both beds is carried away by helium at atmospheric pressure. The First Wall and the other parts of the blanket, made of martensitic steel MANET, are cooled by high pressure helium. Tritium may get to the ambient by

- injection from the plasma into the First Wall and then through permeation to the helium main coolant system;
- permeation from the tritium purging system through the pebble bed containing walls to the helium main coolant system;
- permeation from the helium main coolant system through the walls of the steam generators to the steam turbine cycle.

The permeation from the first wall is of great importance as it represents a relevant source of tritium contamination [2,3]. In the present paper will be studied the influence of a first wall protective layer of beryllium on the corresponding permeation and inventory.

2. HCPB TBM-I first wall design

The HCPB Test Blanket Module (TBM-I) represents a poloidal portion of the HCPB–DEMO blanket, Fig. 1.

Some main characteristics of this first wall design, for which a tritium permeation assessment was done, are briefly here put together:

- pulsed operation incident flux equal to 1×10^{20} ions/$m^2 \times s$ with 1000 s pulses and 1200 s plasma dwell time;
- a 5 mm thick coating layer of beryllium for a first wall of MANET, a martensitic steel initially foreseen for the DEMO reactor. This is a fully martensitic

* Tel.: +49-7247 824 696; fax: +49-7247 825 987; e-mail: luciano.berardinucci@inr.fzk.de.

0022-3115/98/$19.00
PII: S0022-3115(98)00116-0

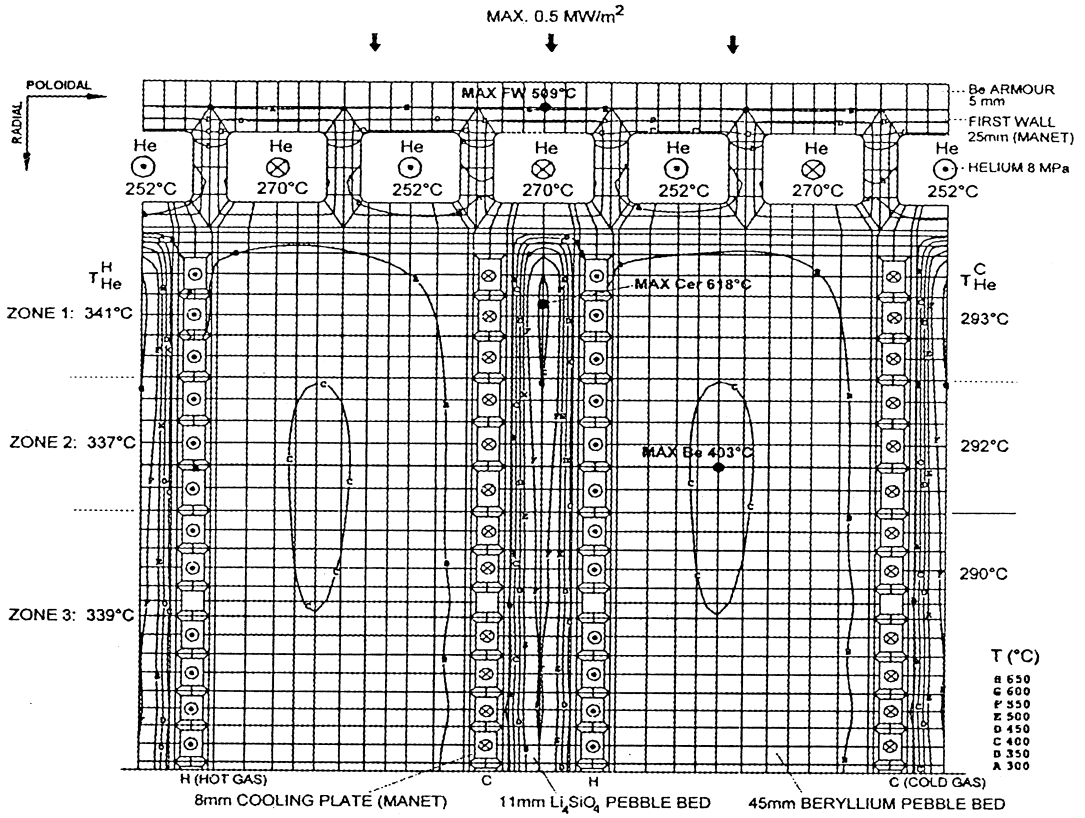

Fig. 1. Radial-poloidal section of the first wall and blanket in the TBM-I.

steel containing 10–11% Cr and additions of approximately 0.6% Mo, 0.65% Ni, 0,25% V and 0.15% Nb;
- a neutron load of 0.5 MW/m^2 has been assumed;
- the maximal temperature in the first wall reaches 782 K.

In Fig. 1 a radial-poloidal section of the Test Module shows the local temperature distribution. To take account of the contribution to permeation of the helium channels lateral walls a two-dimensional assessment has been performed as in Ref. [2].

3. Hydrogen plasma interactions with beryllium surfaces

A first approach to the topic of the tritium permeation through beryllium as plasma facing material for a ITER-like device was made in Ref. [2]. There it was assumed a low porosity (pitting) inside the beryllium during ion implantation. In comparison with the case of a recombination-limited model, the pits result in a reduction of permeation by more than a factor of three and an increase in the time delay to breakthrough by a similar amount [2,3]. This modelling technique involves the creation of a fictitious volume between the disturbed surface layer where the pitting occurs and the relatively undisturbed beryllium matrix [4]. It resulted in a permeation of about 9 mg/d for the total FW surface of the Test Module of 1.2 m^2 [2]. The total inventory in the First Wall (about 1.8 g) is almost completely retained in the beryllium.

A good number of experiments [5–9] have shown a high release rate at the plasma facing surface of beryllium, caused by open porosity in the near-surface area. This suggests not only that retention and permeation through beryllium are controlled by mechanisms other than normal diffusion and surface recombination but also that the considered low porosity approach leads to a high permeation estimate.

When hydrogen is deposited in Be by implantation, the hydrogen collects in bubbles, eventually growing to form interconneted porosities opening to the surface. Once such porosities open, there is virtually no more uptake of hydrogen. Implanted ions very quickly find a free surface where they recombine and return to the plasma [8,9]. Damage caused by the incident ions is not confined to the implantation zone but extends several micrometers deeper, propagated apparently by the diffusion and agglomeration of defects. Experiments are needed nevertheless to determine the depth dependence of tritium concentration in the bulk material. Most hydrogen in ion-implanted Be resides in bubbles and exists

in the molecular form. A smaller amount is combined with vacancies and impurity inclusions such as oxides. An other interesting experimental observation is that gas pressure in the bubbles is nearly equal to the yield strength of the material. Under the plasma conditions considered here, it appears that when the implantation layer has become saturated, essentially all of the implanting flux returns to the upstream face through the cracks and open porosity that it develops. Hence the relative independence on implantation flux.

Finally, under plasma conditions considered in this paper, erosion is serious concern and must be taken account of in any dynamic modelling of the process.

4. Computational method and results

The one-dimensional computer code TMAP4 [10], already used in the previous approach to the study of permeation through beryllium [2,3], has been used for computations referring to the HCPB TBM-I design.

The 5 mm thick coating layer of beryllium was modelled as three segments in series (Fig. 2). The first 50 nm thick segment represents the implantation region, i.e., where most of the bubbles are. It was assumed that they are as a trap concentration of 8% and a trapping energy of 2.2 eV, i.e. the formation enthalpy for diatomic hydrogen molecules. Experimental data [5,6] observed molecular hydrogen saturation already at 6.5%. Achieved the saturation of mobile hydrogen isotopes in Be, the pressure in the bubbles becomes very close to metal yield strength.

A second region 1 μm thick represents a zone of damaged beryllium influenced by the bubbles, characterised by a 0.1% trap at 0.95 eV. In the remaining part of beryllium takes place the process of diffusion. The traps concentration amounts to 0.06% at 0.95 eV trapping energy.

4.1. Modelling of saturation effects

As mentioned before, the bubbles generated by hydrogen implanted into beryllium agglomerate and move to grain boundaries where they coalesce to form surface-connected porosity. This results in a saturation effect that limits the entry of further hydrogen into the beryllium. Once porosity develops, the driving potential for diffusion to the bulk is the gas pressure in the bubbles, which is temperature dependent. Bubble pressure at the saturation reaches approximately the value of the material yield strength, given by

$$S_y = \frac{355\ \text{MPa}}{1 + 0.0012T + (T/950)}.$$

To accommodate the saturation effects on the plasma side of beryllium, the recombination coefficient (K_s) has been modified, thus allowing a recombination-like boundary condition in the TMAP4 input file. The resulting equation for K_r , which grows exponentially when the surface concentration reaches the saturation level, is

$$K_r = \left[3.4E-29\ \exp\left(\frac{-0.28\ eV}{kT}\right)\right]\left[1+\exp\left(\frac{20n_0}{n_{sat}}-1\right)\right]+\frac{u}{1+n_0}\quad\left[\frac{m^4}{s}\right].$$

The first term in brackets is the Hsu–Andrew–Causey value [11], the second one accomplishes the exponential growth where n_{sat} is the concentration saturation value and n_0 that on the boundary; the third one finally takes into account the loss of hydrogen due to surface erosion.

The term n_{sat} has been defined in two ways. The first one as product of the solubility and the square root of the material's yield strength, where for solubility the Shapolov–Dukel'ski value [12] has been used:

$$S = 2.176\times10^{22}\ \exp(-0.17\ eV/kT)\quad[\text{at.}/\text{m}^3\text{Pa}^{1/2}].$$

A better interpolation of available experimental data for the range of temperatures in the TBM-I design is given by the following dimensionally inconsistent expression:

$$n_{sat} = \frac{S_y^{1/2}}{D}(\phi\partial)^{2/3},$$

where S_y is the yield strength in MPa, ϕ is the ion flux to the surface in ion/m^{2}s and δ is the implantation depth in m.

For diffusivity D Abramov's "extra-grade" value has been used for the first segment to account for the greater transport expected due to vacancy and dislocation movements. The "high-grade" value has been assumed for the rest of beryllium [13].

4.2. Modelling of surface erosion

Erosion due to sputtering results in a diffusion in a moving coordinate system. Hydrogen atoms in the

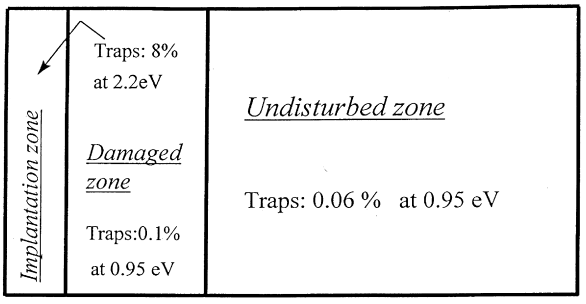

Fig. 2. Structure assumed in modelling permeation through Be.

eroded layer leave along with the eroded matrix atoms. The diffusion equation used for atom flux J_i through the matrix of beryllium is:

$$J_i = -D\left(\nabla n_i + \frac{n_i Q^*}{kT^2}\nabla T\right),$$

where D is the diffusivity, n_i the concentration of atoms, k is Boltzmann's constant, T is the temperature and the second term in parentheses accounts for the Soret effect [14], i.e., the mass transport due to a temperature gradient, characterised by the heat of transport Q^*. Neglecting Q^* for beryllium, not yet available anyway, we can use the relation:

$$\frac{DQ^*}{kT^2}\nabla T = u,$$

where u is the surface erosion velocity assumed equal to:

$$u = \frac{\phi\eta}{N}$$

being η the sputter coefficient (taken as 3×10^{-3}) and N the lattice concentration (Fig. 3). In this way the diffusion equation is as follows:

$$J_i = -D\,\nabla n_i - u n_i,$$

where u is positive in the positive x direction. The total flux of mobile hydrogen ions to the surface can be also written as:

$$J_i = -(2K_r n_{i0}^2 + u n_{i0})$$

being n_{i0} the boundary atoms concentration: the recombination current is in the negative x direction for positive u values.

Erosion was included only in the damaged zone (first and second segment of Be). The reduction of the beryllium thickness, leading to a lower inventory and higher permeation, was accounted for by an iterative procedure. At fluxes higher than 10^{20} ions/m^{2}s it may be that beryllium of the implantation zone is eroded away faster than the bubbles can form.

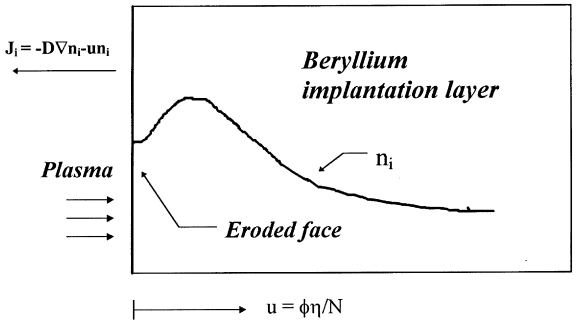

Fig. 3. Modelling of surface erosion in TMAP4.

4.3. Results

Total operational time was given as 6×10^6 seconds, i.e. about 70 days. An accurate thermal calculation has been performed for each modelled segment. For the assumed first wall surface of 1.2 m^2 and the whole operating period, a permeation of about 0.007 g has been obtained. This very low permeation is not appreciably influenced by the use, instead of MANET, of a ferritic steel like T91. In the case of non-protective layer the permeation after 70 days would be of at least one gram [2].

Data concerning the spatial distribution of the implanted ions and the diffusivity in the implantation region need to be correctly evaluated, as they may influence the resulting permeation appreciably.

5. Conclusion

With a coating layer of beryllium, the permeation through the HCPB TBM-I first wall is strongly reduced, so that it can be neglected. As far as the permeation is concerned, the choice of the steel to be used together with beryllium does not play an important role. As the permeation from the orthosilicate (Li_4SiO_4) pebble beds in the blanket has been also adequately reduced (equal to 0.3 mg/d), the HCPB TBM-I design complies with ITER safety criteria.

What remains to be modelled is the influence of carbon on the retention and permeation of beryllium-clad surfaces. There are not many data available about how much of the carbon that will be sputtered from high-heat-flux surfaces in the divertor will be transported to the main plasma chamber and end up on the first wall, where carbon film build-up may be probable. The hydrogen implantation in the first wall seems in any case to be significant at depths, that result in development of the described open porosity. The highly erosive action of the plasma should keep the plasma-facing surfaces quite clean of contaminants films.

Acknowledgements

The author thanks Dr. Glen Longhurst for his important contribution to this paper and his constant encouragement. His helpful comments and suggestions have contributed to the understanding of important aspects of the phenomena described here and to the solving of several numerical problems.

References

[1] FZKA 5891, Forschungszentrum Karlsruhe, Design Description Document, HCPB Test Blanket, 1996.

[2] L. Berardinucci, M. Dalle Donne, in: Proceedings of 19th SOFT, Lisbon, Portugal, 16–20 September, 1996, pp. 1427–1430.
[3] FZKA 5858, Forschungszentrum/EURATOM, Nuclear Fusion Project, Annual Report, 1997.
[4] D.F. Holland, G.R. Longhurst, Fusion Technology 8 (1985) 2067.
[5] M.I. Guseva, A.Yu Birukov, V.M. Gureev, L.S. Daneljan, S.N. Korshunov et al., J. Nucl. Mater. 233–235 (1996) 681.
[6] V.N. Chernikov, V.Kh. Alimov, A.P. Zakharov et al., J. Nucl. Mater. 233–237 (1996) 860.
[7] A.A. Haasz, J.W. Davis, J. Nucl. Mater. 241–243 (1997) 1076.
[8] W.R. Wampler, J. Nucl. Mater. 196/197 (1992) 981.
[9] W.R. Wampler, J. Nucl. Mater. 122/123 (1984) 1598.
[10] G.R. Longhurst et al., TMAP4 User's Manual, INEL, EGG-FSP-10315, 1992.
[11] R.A. Causey, K.L. Wilson, J. Nucl. Mater. 212–215 (1994) 1436.
[12] V.I. Shapovalov, Yu.M. Dukel'ski, Russian Metallurgy 5 (1984) 201.
[13] E. Abramov et al., CFFTP-G-9013, Canadian Fusion Technology Project, Mississauga, Ontario, Canada, 1990.
[14] G.R. Longhurst et al., J. Nucl. Mater. 131 (1985) 61.